Available online at www.sciencedirect.com

ScienceDirect

Geochimica et Cosmochimica Acta 127 (2014) 67–82

Geochimica et Cosmochimica Acta

www.elsevier.com/locate/gca

Zn isotope compositions of the thermal spring waters of La Soufrière volcano, Guadeloupe Island

Jiu-Bin Chen [a,b,*], Jérôme Gaillardet [b,e], Céline Dessert [b,c], Benoit Villemant [d], Pascale Louvat [b], Olivier Crispi [c], Jean-Louis Birck [b], Yi-Na Wang [a]

[a] State Key Laboratory of Environmental Geochemistry, Institute of Geochemistry, Chinese Academy of Science, Guiyang 550002, China

[b] Institut de Physique du Globe de Paris (IPGP), Université Paris-Diderot, Sorbonne Paris Cité, CNRS (UMR 7154), 1 rue Jussieu, 75238 Paris cedex 05, France

[c] Observatoire Volcanologique et Sismologique de Guadeloupe (OVSG), IPGP, Université Paris-Diderot, Sorbonne Paris Cité, 97113 Gourbeyre, Guadeloupe

[d] Equipe de Volcanologie, IPGP & ISTeP, CNRS (UMR 7193), UPMC Université Paris 6, 4 pl. Jussieu, 75252 Paris, France

[e] Institut Universitaire de France

Received 11 May 2013; accepted in revised form 16 November 2013; available online 25 November 2013

Abstract

To trace the sources and pathways of Zn in hydrothermal systems, the Zn isotope compositions of seventeen water samples from eight thermal springs and six gas samples from two fumaroles from La Soufrière, an active volcano on Guadeloupe Island (French West Indies, FWI), were analyzed using a method adapted for purifying Zn from Fe- and SO_4-enriched thermal solutions. The fumaroles are enriched in Zn 100 to 8000 times compared to the local bedrock and have isotopic compositions (δ^{66}Zn values from +0.21‰ to +0.35‰) similar to or slightly higher than fresh andesite (+0.21‰). The enrichment of Zn in the thermal springs compared with the surface waters shows that Zn behaves as a soluble element during hydrothermal alteration but is significantly less mobile than Na. The δ^{66}Zn values of most of the spring waters are relatively constant (approximately 0.70‰), indicating that the thermal springs from La Soufrière are enriched in heavy isotopes (i.e., ^{66}Zn) compared to the host rocks (from −0.14‰ to +0.42‰). Only three thermal springs have lower δ^{66}Zn values (as low as −0.43‰). While the Zn in the fumaroles is essentially derived from magma degassing, which is consistent with a previous study on Merapi volcano (Toutain et al., 2008), we show that the Zn in the thermal springs is mainly derived from water–rock interactions. The ^{66}Zn-enriched isotopic signature in most of the spring waters can be explained qualitatively by the precipitation at depth of sulfide minerals that preferentially incorporate the light isotopes. This agrees with the isotopic fractionation that was recently calculated for aqueous complexes of Zn. The few thermal springs with lower δ^{66}Zn values also have low Zn concentrations, indicating the preferential scavenging of heavy Zn isotopes in the hydrothermal conduits.

This study shows that unlike chemical weathering under surface conditions, hydrothermal alteration at high temperatures significantly fractionates Zn isotopes and enriches thermal waters in heavy Zn isotopes (e.g., ^{66}Zn). Continental hydrothermal systems therefore constitute a source of heavy Zn isotopes to the oceans; this should be taken into account in the global oceanic budget of Zn.

© 2013 Elsevier Ltd. All rights reserved.

* Corresponding author at: State Key Laboratory of Environmental Geochemistry, Institute of Geochemistry, Chinese Academy of Science, Guiyang 550002, China. Tel./fax: +86 851 5892669.

E-mail address: chenjiubin@vip.gyig.ac.cn (J.-B. Chen).

0016-7037/$ - see front matter © 2013 Elsevier Ltd. All rights reserved.
http://dx.doi.org/10.1016/j.gca.2013.11.022

1. INTRODUCTION

The intense hydrothermal activities of active volcanoes are visible at the Earth's surface in the form of fumaroles, hot springs, and specific minerals and condensates, especially in equatorial regions. Thermal springs of active volcanoes are monitored because they provide a rare window on hydrothermalism. Changes in the chemical composition of thermal springs may be an accurate tool for the prediction of volcanic activities. Moreover, thermal waters play a pivotal role in the global cycling of elements at the surface of continents because the complex interactions between meteoric water, aquifers, seawater, magmatic fluids and bedrock under high heat flow conditions favor the release of cations and metals. These reactions may result in a large flux of elements to the ocean (Louvat and Allègre, 1997; Varekamp and Thomas, 1998; Dessert et al., 2003, 2009; Gaillardet et al., 2011a,b; Schopka et al., 2011). The study of thermal waters in volcanic regions is also critical for assessing geothermal energy resources. Several tracers have been proposed for monitoring the hydrothermal activity of active volcanoes, including temperature and major elements (e.g., Brombach et al., 2000; Joseph et al., 2011; Villemant et al., 2005), conventional H, O, and C isotopes (e.g., Chiodini et al., 2000; Caliro et al., 2005), and newly developed B, Sr, Pb and noble gas isotopes (Pedroni et al., 1999; van Soest et al., 1998; Nonell et al., 2005; Pennisi et al., 2000; Ruzié et al., 2012; Louvat et al., 2011). Other isotopic systems have also been used to constrain water–rock interactions and the origin of elements in geothermal fields (e.g., Aiuppa et al., 2000b; Cortecci et al., 2001; Leeman et al., 2005; Millot et al., 2010). These studies demonstrate the potential of isotopic tracers for investigating the hydrothermal features of active volcanoes and for quantifying the contribution of hydrothermal activity to surface waters and the ocean.

Zinc isotopes may be used as a tracer. Zn is a transition metal that is volatile at high temperatures and thus is generally enriched in the gas, aerosols and condensates in volcanic systems (Cloquet et al., 2008; Toutain et al., 2008; Mattielli et al., 2009). The annual global volcanic flux of Zn is approximately 6500 tons/year (Lambert et al., 1988; Gauthier and Le Cloarec, 1998), which represents a major source of Zn in the surface environment. However, the behavior of Zn in hydrothermal systems is poorly understood. Aiuppa et al. (2000a,b) reported on the Zn concentrations in the groundwater of Mt. Etna in Sicilia (Italy) and demonstrated that Zn has an intermediate behavior between the most mobile elements, such as Na, and the least mobile elements, such as Al. The only available data on Zn isotopes in hydrothermal systems are related to seafloor vent fluids, hydrothermal ore deposits and fumarolic gas (Mason et al., 2005; Wilkinson et al., 2005; John et al., 2008; Toutain et al., 2008; Gagnevin et al., 2012). These studies, along with low-temperature surface water investigations (Chen et al., 2008, 2009a), report large isotopic variations for Zn and therefore demonstrate the reason for the interest in Zn isotopes for investigating water–rock interactions and hydrothermalism. However, to the best of our knowledge, the Zn isotopes in continental thermal water systems have not been investigated yet.

The challenge in measuring the Zn isotope compositions of thermal water is the low Zn concentrations (a few to several tens μg/L). Large volumes of water are thus needed to retrieve sufficient amounts of Zn (typically 1 μg) for precise isotopic analyses (at least four replicates). Moreover, to make accurate Zn isotopic measurements, the Zn from the solution matrix must be thoroughly purified, particularly from elements such as Cu, Ni, Co, and Cd (Borrok et al., 2007; Chen et al., 2009b). Ion-exchange purification on AG-MP1 resin (Marechal et al., 1999; Borrok et al., 2007; Chen et al., 2009a) is thus difficult to apply to dilute thermal waters due to the requirement of either (or both) the evaporation of large amounts of water or the addition of large volumes of acid (inducing a high pH). In a previous paper, we presented a method of purifying Zn from dilute water samples and applied it to river samples containing less than 10 μg of Zn per liter (Chen et al., 2009b). However, the first tests using this method demonstrated that this protocol could not be applied to thermal waters. Although the low Zn concentrations of thermal springs are expected to be in the same range as rivers, thermal waters generally contain high concentrations of elements and chemical compounds such as Fe, Mn, Al, and SO_4. Sample loading at a relatively high pH = 5.5 led to the rapid precipitation of a mix of hydroxides in the first layer of the Chelex-100 resin due to redox changes and could even stop the introduction flux. This would also induce the co-precipitation of Zn and possible isotopic fractionation (Bau et al., 1998; Cheynet et al., 2000). Therefore, a new separation method had to be developed to purify Zn from thermal waters.

In this paper, we developed a one-step retrieval method for purifying Zn from dilute thermal water samples that was adapted for isotopic measurements. The protocol was validated by multiple tests using several eluates and Zn concentrations of the loading solutions and by checking the complete recovery of Zn and estimating the reproducibility of the measured isotopic compositions. The method was applied to 17 spring water samples from the La Soufrière volcanic system on the island of Guadeloupe (French West Indies, FWI) with dissolved Zn concentrations between 1 and 33 μg/L. These waters display a large range of isotope variations that are similar to those that have been reported for hydrothermal systems and are systematically enriched in heavy Zn isotopes compared with the parent bedrocks. This paper discusses using Zn isotopes to identify the controls on Zn isotope fractionation in thermal water systems and to investigate the hydrothermal circulation in active volcanoes.

2. EXPERIMENTAL SECTION

2.1. Geological setting and sampling

The sampling site is located on Basse Terre Island (Guadeloupe archipelago, French Lesser Antilles), a volcanic arc island formed by the subduction of the Atlantic Plate beneath the Caribbean Plate (Fig. 1). Thermal spring waters were collected on the slopes of La Soufrière volcano, one of the dozen active explosive-type volcanoes in the most recent Caribbean volcanic arc. La Soufrière volcano is

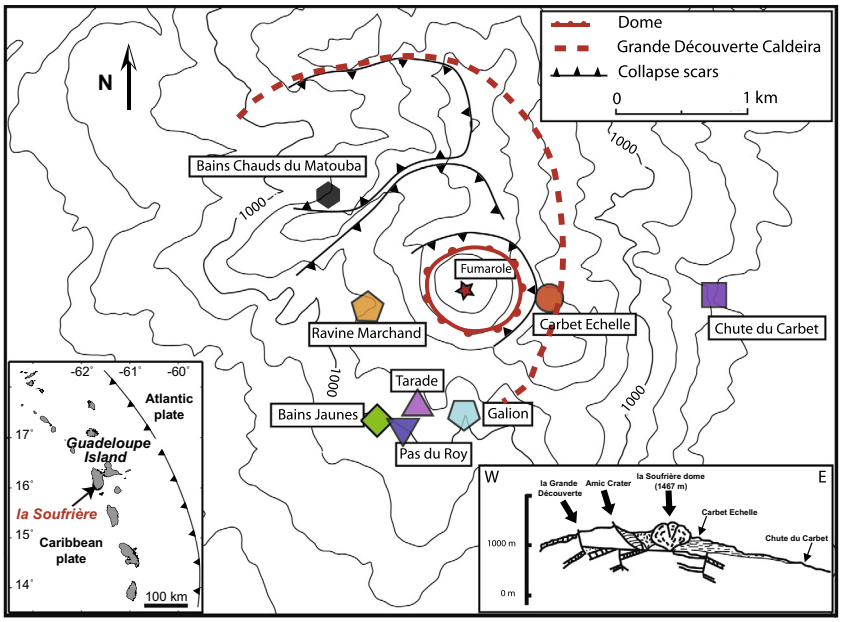

Fig. 1. Map of La Soufrière volcano and sampling locations (modified from Ruzié et al., 2012). CE, GA, BJ, RM, PR, TA, CC, and BCM represent the Carbet Echelle, Galion, Bains Jaunes, Ravine Marchand, Pas du Roy, Tarade, Chute du Carbet, and Bains Chauds du Matouba thermal springs, respectively.

located in the southern part of Basse Terre Island and belongs to the Grande-Découverte/Soufrière composite volcanic complex, which began erupting at 0.2 Ma. The most recent phase, which is still active, began during the Holocene and is characterized by a succession of lava dome eruptions. The most recent eruption, which formed the present basaltic–andesitic lava dome of La Soufrière, has been dated at 1530 AD (Boudon et al., 2008; Samper et al., 2009). The last phreato-magmatic eruption occurred in 1976. The dominant pyroclastic and lava flow rock types are andesitic. High-pressure acid degassing at the summit and thermal springs on the slopes of La Soufrière are the main signs of intense hydrothermal activity. Basse Terre Island has a tropical climate that is characterized by relatively high temperatures (24–32 °C), very dense vegetation, and pronounced relief (Rousteau, 1996; Lloret et al., 2011). The precipitation rate is approximately 10 m per year at the summit of La Soufrière and decreases to 2.5 m/year at the coast.

Water samples from eight thermal springs were collected within a 4 km radius of the La Soufrière lava dome (Fig. 1). Six surveyed springs are located at high elevations (950–1150 m) in the Amic crater within 1.2 km of the dome's summit: Carbet Echelle (CE), Galion (GA), Bains Jaunes (BJ), Ravine Marchand (RM), Pas du Roy (PR) and Tarade (TA). The Chute du Carbet (CC) spring is located at a lower elevation (590 m) and is further away from the dome summit but is likely related to the Amic crater hydrogeological system (Villemant et al., 2005; Fig. 1). The Bains Chauds du Matouba (BCM) spring is located at a lower elevation and is outside the Amic crater; it is independent of the actual active dome system. The distribution of these thermal springs is controlled by the internal volcanic structure and important hydrothermal clay formation in the upper layer (Brombach et al., 2000; Villemant et al., 2005). Previous studies provide a detailed description of the mineralogy, the eruption activity, and the structure of the lava dome (Zlotnicki et al., 1992; Macdonald et al., 2000; Nicollin et al., 2006; Zlotnicki et al., 2006; Boudon et al., 2008; Salaün et al., 2011). Except for the TA spring, all of the springs have relatively constant flow rates that range from 3 to 140 L/min (annual report of the Volcanic Observatory of Guadeloupe (OVSG), IPGP). Physico-chemical monitoring of these thermal springs has been performed by the OVSG since 1979 after the 1976–1977 seismo-volcanic crisis at La Soufrière (Feuillard et al., 1983; Hirn and Michel, 1979; Villemant et al., 2005). The increasing fumarolic activity since 1992 and HCl degassing since 1998 prompted the observatory to increase the surveillance of the volcano. The 30-year monitoring of major dissolved elements has shown that the chemical composition of the thermal springs only varies on a multiyear timescale. Based on this finding, the spring waters were sampled two to four times between 2007 and 2011 to assess the temporal variation of Zn concentration and isotopic compositions.

Six fumarolic gases were also sampled in 2010 from two active fumaroles: one in the south-center crater (CSC) and the other in the south-north crater (CSN) of La Soufrière dome (see locations in Nicollin et al., 2006). These gases were collected through a 7.5 m-long tube followed by complete condensation into a container. The condensed solution is thus representative of the fumarolic gas. These fumarolic gases have an average temperature of approximately 98 °C and are mostly composed of H_2O vapors (93–97%) with small amounts of CO_2, H_2, H_2S, and traces of CH_4, CO, N_2, and volatile metal

species (Brombach et al., 2000; Bernard et al., 2006; OVSG comments). Two river water samples from the Bras-David River (BD) and the Capesterre River (CP) were also collected for Zn isotope measurements (see Lloret et al., 2011 for the river locations). The sampling set was complemented by bedrock materials, including one fresh andesite sample (1530 AD dome fragment E1215; Boudon et al., 2008), one pyrite sample that was collected from a road cut at the Col des Mamelles, one gypsum sample from the dome, two Fe(Mn) oxyhydroxides that precipitated around the Galion spring orifice, and five andesitic rocks that were altered to varying degrees (in order of increasing degree of alteration: two highly altered rocks, R805 and R825, and three rock samples, 23CF, 31S and 71S, from a core at the dome summit; see Salaün et al., 2011 for details).

2.2. Materials and sample preparation

Milli-Q water (18.2 MΩ resistivity, Millipore) was used throughout the chemical procedures. The HCl and HNO_3 acids were purified by sub-boiling distillation. Double distillation was performed for the concentrated HCl to reduce the Zn blank measured at 34 ng/L after the first distillation. The elemental blanks of reagents were determined (at least three times) with a Neptune MC-ICP-MS after evaporation of 10 ml of the initial solution. The elemental blank concentrations were 1.0, 5.0, and 3.1 ng Zn/L for the distilled water, concentrated HNO_3 and double-distilled HCl, respectively. The concentrated HCl and HNO_3 were diluted to 2 M HCl, 0.1 M HCl, 2 M HNO_3, 0.5 M HNO_3 and 0.05 M HNO_3 solutions for Zn purification. Cu-SRM976 and Zn-JMC3-0749L were used as international reference materials. The AAS Zn standard (1000 mg/L, Alfa Aesar, Germany) was used as an in-house isotopic standard and to assess Zn isotopic fractionation during chemical separation (Chen et al., 2009b). All of the vials were cleaned with ultra-pure HNO_3 and were rinsed with Milli-Q water just before their use.

The spring water samples were filtered after sampling through pre-cleaned ($HNO_3 + H_2O$) 0.2-μm-porosity filter membranes at IPGP (Chen, 2008, 2009b). The aliquots of filtered water used for anion analysis were not acidified. The water samples for the cation concentration and Zn isotopic measurements were acidified to pH = 2 with distilled HNO_3 (15 M) and HCl (6 M), respectively. The fumarole gases (condensates) were centrifuged to discard the small amount of solids, and the solution was prepared for further Zn chemical separation and isotopic measurements. The major elements (Na, K, Mg, Ca, Cl, and SO_4) were measured by ion chromatography (Dionex DX120) at OVSG with uncertainties less than 3%. The concentrations of trace elements in the solutions were measured with an ICP-MS (Thermo X-series II) at Pierre and Marie Curie University. The analytical quality of the elemental concentration measurements was improved by the addition of internal standards (In and Re) and was controlled by regular measurements of the international river water geo-standard SLRS4. The precision for the trace element concentrations was generally better than 5%.

Element concentrations were also measured for complementary solid samples after acid digestion (Chen et al. 2009a).

2.3. One-step separation of Zn from Fe(SO_4)-enriched thermal water

The AG1-X4 anion-exchange resin (200–400 mesh, Bio-Rad) was used in this study for Zn purification. The resin has R-$CH_2N^+(CH_3)_3$ functional groups that display a strong affinity for the Zn complex in HCl (e.g. $ZnCl_4^{2-}$; Trémillon, 1965). The resin was carefully washed and settled in water to discard the finer grains before packing the column.

In this study, a one-step purification method was developed based on the separation protocol reported in John et al. (2008). The detailed elution sequence is summarized in Table 1. A polypropylene column (volume 11 ml, reservoir diameter 1.7 cm, height 10 cm, Bio-Rad) was packed with the previously prepared AG1-X4 resin. Considering the Zn partition coefficient (Kd) at 2 M HCl (>2000) and the possible competition effect due to the high concentrations of other elements, the resin volume was fixed at 1 ml (Trémillon, 1965). The introduction flow rate was controlled by gravity and was an average of 0.75 ml/min; thus, a long time was required for large amounts of dilute water samples to pass through the column and accumulate a sufficient mass of Zn. After sample introduction, 10 ml of 2 M HCl solution was introduced for matrix rinsing. The reagents HNO_3, H_2O, HBr and HCl were tested for eluting Zn from the resin. Zn generally displays lower Kd values (i.e., <10) in dilute HNO_3, HBr, HCl and water solutions (Trémillon, 1965). Preliminary tests demonstrated that Cd, which may interfere with Zn isotope measurements (Borrok et al., 2007), was not separated from Zn when using HNO_3 or H_2O as eluates. For Zn elution with 0.2 M HBr, most of the Zn was eluted within the first 10 ml, but a small amount was still observed in the subsequent washing solution (0.05 M HNO_3), leading to an overlap with the Cd peak. Finally, 0.1 M HCl was chosen to elute Zn because it led to a sharper and better-separated peak than the 0.25 and 0.5 M HCl did. The elution volume was fixed at 10 ml, and the elution rate was set at approximately 0.3 ml/min by controlling the eluent loading rate.

Fig. 2a shows the elution process of Zn separation from a thermal spring water sample (CE-2). Compared with the elemental concentrations measured before loading the sample, the major elements (i.e., Na, and Mg) passed directly through the column, whereas trace elements such

Table 1
Elution sequence of the one-step separation of Zn from hydrothermal water using 1 ml AG 1×4 Bio-rad resin (200–400 mesh).

Eluent	ml	Eluted
2 M HNO_3	10	Cleaning
H_2O	10	Rinsing
2 M HCl	5	Conditioning
Sample loading in 2 M HCl	up to 1 L	Loading
2 M HCl	10	Matrix
0.1 M HCl	10	Zn

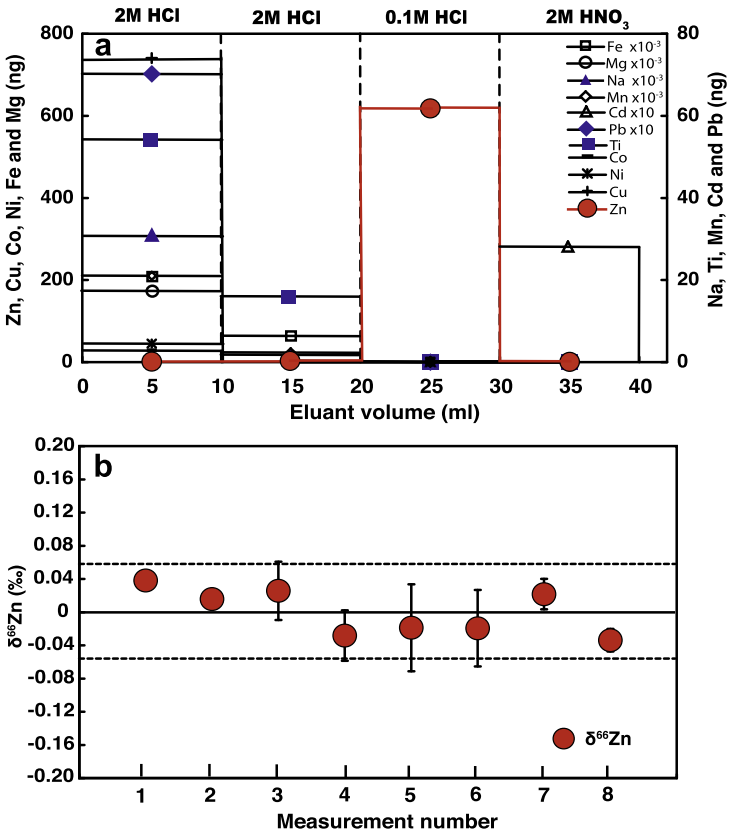

Fig. 2. Elution scheme of Zn separation from the thermal spring water sample CE-2 on AG 1×4 resin (a), and the reproducibility of δ^{66}Zn in elution fractions from eight chromatographic separation tests on column-purified (Zn removed) spring waters spiked with the AAS Zn standard (b). (a) Shows that Zn is separated from the major and trace elements. In (b), the isotopic composition of Zn in the elution fractions is similar to that of the Zn loaded onto the column.

as Cu, Ni, Co, Cr, Pb, V, Fe, Mn and Ti were not retained by the resin or were only partially detected in the first rinsing fraction before Zn elution. Cd was only observed in the washing fraction after Zn elution. The total Zn blank of the separation chemistry was tested by loading 50–200 ml of distilled water and was approximately 3.4 ± 0.8 ng ($n = 5$). Because the typical quantity of Zn needed for the isotope analysis is 1 μg (Chen et al., 2009b), no significant influence of this blank is expected on natural samples. The yield for the chemical separation was determined to be approximately 100% for all of the water samples by comparing the Zn concentrations in the eluates (measured by Neptune ICP-MS) with those measured before sample loading.

To estimate the separation reproducibility and to verify that the chemical procedure did not cause isotopic fractionation of Zn, Zn isotopes were measured in eight solutions that were generated from the separation tests on column-purified (to remove Zn) spring waters spiked with the AAS Zn standard. The δ^{66}Zn of the final elution fractions varied from $-0.03‰$ to $+0.04‰$ with an average value of $0.00‰ \pm 0.06$ (2σ standard deviations; Fig. 2b), which is identical, within the uncertainties, to that of the Zn loaded onto the column. Repeated separations (11 times) of sample CE-2 also validated the protocol (see Section 2.4). Finally, chemical separation of Zn was performed using a previously reported protocol with AG MP1 resin (Chen et al., 2009a) on an evaporated Zn-enriched sample (29 μg/L, CE-2); the measured Zn isotopic ratio ($+0.73‰ \pm 0.07$, 2σ) is consistent with that obtained using our new separation method using AG1-X4 resin ($+0.74‰ \pm 0.06$, 2σ).

2.4. Zn isotope measurement by MC-ICP-MS

The Zn elution fractions from the chemical separation of the water samples were evaporated and re-dissolved in 0.05 M HNO_3 for isotopic measurements. The Zn isotopic compositions of solid samples were also measured after digestion and Zn extraction using the chromatographic method reported in Chen et al. (2009a).

The measurement of Zn isotope compositions was described in detail by Chen et al. (2009b). The Zn isotopic analyses were performed on a Neptune MC-ICP-MS (Thermo Finnigan®, Germany) at IPGP using an Apex HF desolvator (ESI) with a 50 μl/min micro-concentric nebulizer as the introduction system. All of the solutions were measured in 0.05 M HNO_3 at a Zn concentration of 200 μg/L, which resulted in a signal of approximately 10 V for ^{64}Zn (10^{11} Ω amplifiers). The international Cu standard SRM976 was added to both the Zn sample and the bracketing standard solutions as an internal standard with a Zn/Cu elemental ratio of 2. Simultaneous measurements of the Zn and Cu isotopes allowed for the correction of the instrumental mass bias according to the modified 'empirical

Table 2
Elemental concentrations and Zn isotopic composition of hydrothermal spring waters and fumarolic gases of La Soufrière volcano system.

	n	Sample	Date	$\delta^{66}Zn$	*T* (°C)	pH	Discharge (L/min)	Cl (mg/L)	SO_4 (mg/L)	HCO_3 (mg/L)	Na (mg/L)	Mg (mg/L)	K (mg/L)	Ca (mg/L)	Sc (μg/L)	Ti (μg/L)	V (μg/L)	Mn (μg/L)	Fe (μg/L)	Cu (μg/L)	Zn (μg/L)
TA-1	4	Tarade	2007-9-26	-0.14 ± 0.05	39	6.6		109	487	95	83	48	16	134	18	11	48	56	536	2	4
TA-2	3	Tarade	2008-5-15	0.09 ± 0.05	39	6.1	85	160	734	102	96	75	19	219	20	12	30	51	856	2	4
TA-3	8	Tarade	2011-3-30	1.01 ± 0.06	39	5.9	87	146	778	119	93	66	19	222	18	13	22			2	1
CE-1	7	CarbetEchelle	2007-9-26	0.72 ± 0.03	21	5.7	4	20	791	55	29	47	6	192	65	33	4420	11,597	120,000	11	29
CE-2	11	CarbetEchelle	2007-10-11	0.74 ± 0.06	21	5.5	4	13	762	66	31	50	6	192	70	37	3430	11,164	126,000	12	29
CE-3	7	CarbetEchelle	2008-5-15	0.67 ± 0.05	21	5.4	3	13	806	53	28	48	6	206	75	34	3180	11,469	122,000	11	33
CC-1	4	Chute du Carbet	2007-9-27	0.25 ± 0.04	44	6.8		134	241	155	83	42	20	86	22	11	117	1	375	1	4
CC-2	4	Chute du Carbet	2011-4-5	0.31 ± 0.07	45	6.8		106	214	160	69	33	17	74	10	10				1	3
PR-1	7	Pas du Roy	2007-10-11	0.63 ± 0.04	34	5.7	5	61	489	53	62	47	11	144	24	12	68	1568	3820	2	9
BCM-1	4	Matouba	2008-5-20	-0.43 ± 0.02	59	5.8		22	714	23	34	13	8	253	8	3	3	797	1150	2	2
RM-1	7	Ravine Marchand	2007-10-31	0.68 ± 0.06	43	5.4	22	61	501	74	48	38	16	142	31	18	68	3176	17,200	2	15
RM-2	7	Ravine Marchand	2008-6-3	0.68 ± 0.03	43	5.4	22	71	495	56	48	40	16	149	32	17	65	3218	13,100	2	15
BJ-1	7	BainsJaunes	2007-9-26	0.60 ± 0.03	31	5.3		50	343	15	41	26	6	98	22	11	65	510	401	2	12
BJ-2	7	BainsJaunes	2007-10-11	0.64 ± 0.03	31	5.4		44	330	15	44	28	7	100	26	11	84	520	399	2	12
BJ-3	7	BainsJaunes	2008-5-15	0.62 ± 0.03	31	5.4		50	370	13	41	28	7	108	28	11	45	446	457	1	12
GA-1	8	Galion	2008-5-15	0.80 ± 0.05	46	4.9	142	305	709	43	64	75	19	281	34	17	58	5450	13,800	2	10
GA-2	5	Galion	2011-3-30	0.54 ± 0.05	46	4.8		464	615	33	69	81	21	314	21	15		5400	16,100	2	8
Capes	3	Capesterre River	2011-3-15	0.29 ± 0.04	21	7.9		5	3	28	6	1	1	5	4	3			75	1	
BD	3	Bras-David River	2011-4-1	0.28 ± 0.08	21	7.7		8	2	32	8	2	1	5	4	3			84		
CSC-1	3	Fumarolic gas	2010-6-22	0.30 ± 0.04				288	2490		15	28	15	134			2		2050	21	201
CSC-1B	3	Fumarolic gas	2010-6-22	0.30 ± 0.04				290	389		22	34	14	137			2		2350	18	13
CSC-2	3	Fumarolic gas	2010-7-13	0.35 ± 0.01					78,000		22	30	17	296			3		3320	46	70
CSC-2B	3	Fumarolic gas	2010-7-13	0.31 ± 0.09				806	557		33	29	18	156			5	4	2900	23	67
CSN-1	3	Fumarolic gas	2010-5-5	0.31 ± 0.09				16,900	2300		25	223	24	521			41	7	361	21	38
CSN-2	3	Fumarolic gas	2010-6-22	0.21 ± 0.08				16,700	2350		83	29	26	168			5	19	2610	25	378

n, number of Zn isotopic measurements; Zn isotope analytical uncertainties are 2 external standard deviations (2σ).

external normalization' method (see Chen et al., 2009b). After signal and peak optimization, the Zn isotope composition was analyzed in a "loose" standard-samples-standard bracketing sequence (one standard measurement every three to four samples). One measurement consisted of 100 integrations of 4.2 s in five blocks of 20 cycles and lasted for 13 min. All of the Zn isotopic results are expressed as $\delta^{66}Zn$ (in ‰):

$$\delta^{66}Zn = [(^{66}Zn/^{64}Zn)_{sample}/(^{66}Zn/^{64}Zn)_{JMC} - 1] \times 1000 \quad (1)$$

where JMC is the JMC3-0749L Zn international standard (Marechal et al., 1999). The error bars in this paper are all 2σ external standard deviations of repeated measurements (at least three times). The quality of the Zn isotope analysis was controlled by regular measurements of the in-house standard AAS Zn (Alfa Aesar, Germany). The long-term calibration measurements of this standard resulted in an external reproducibility of 0.04‰ (2σ) for $^{66}Zn/^{64}Zn$. The spring water sample CE-2 that was measured most frequently (11 times) gave an external 2σ uncertainty of 0.06‰ (Table 2). The international standard BCR-1 basalt (USGS, USA) was also processed and measured, and the average $\delta^{66}Zn$ value of $+0.28 \pm 0.02$‰ (2σ) was consistent with those reported in previous studies (Archer and Vance, 2004; Chapman et al., 2006; Cloquet et al., 2008; Chen et al., 2009a). Overall, the Zn isotope compositions of all of the samples defined a regression line of $\delta^{68}Zn$ vs. $\delta^{66}Zn$ with a correlation coefficient (R^2) of 0.9972. The slope of this line agrees with the mass-dependent fractionation theory at the 95% level (Young et al., 2002; Petit et al., 2008; Chen et al., 2009b). These results indicate that all of the sample purifications were sufficient, and neither residual interference nor counting problems occurred during the Zn isotopic measurements.

3. RESULTS

3.1. Geochemistry of thermal waters

All of the spring waters are slightly acidic and have relatively high temperatures. The pH varies from 4.9 (GA) to 6.8 (CC), and the temperature varies from 21 °C (CE) to 59 °C (BCM). Our data are consistent with previous studies that described the major element geochemistry of thermal spring waters (Bigot and Hammouya, 1987; Bigot et al., 1994; Brombach et al., 2000; Villemant et al., 2005; annual report of OVSG). The dominant ions in the hot springs are SO_4^{2-} and Cl^-, which indicates the contribution of a deep geothermal aquifer that is fed by ascending volcanic gas (Brombach et al., 2000; Nonell et al., 2005). This is a typical characteristic of hydrothermal systems of andesitic volcanoes and particularly of Lesser Antilles volcanoes that produce S- and Cl-rich acid gases (Bernard et al., 2006; Villemant et al., 2008 and references therein). This contrasts with the composition of thermal water samples from Mt. Etna, where all samples display relatively high bicarbonate concentrations (Aiuppa et al., 2000a) that indicate the neutralization of CO_2-rich gases by water–rock interactions.

During the sampling period, springs CE, CC, PR, BCM, RM and BJ displayed a relatively narrow range of concentrations (i.e., <10%) for each major element (Table 2). Between 2008 and 2011, GA had an increase of Cl^- concentration, a decrease of SO_4^{2-} concentration, and relatively constant concentrations of the other major elements (Table 2). These changes may reflect variable contributions from different sources. Significant variations (20–40%) were observed for almost all major elements in TA between 2007 and 2011, with higher Cl^-, SO_4^{2-}, Ca, and Mg concentrations in April than in September (Table 2). These seasonal variations are consistent with the results of long-term observations by the OVSG (http://www.ipgp.fr/pages/0303040901.php). Although all of the spring samples had variable ranges of concentration of major elements, they define linear relationships in the SO_4^{2-}/Na vs. Ca/Na diagram (Fig. 3a). However, in the Mg/Na vs. Ca/Na and SO_4^{2-}/Na diagrams, spring BCM, which is located outside the Amic crater, plots off the linear relationships defined by all of the other springs (Fig. 3b and c), indicating the enrichment of Ca and SO_4^{2-} in this spring.

The spring waters of BCM, CC, and TA have the lowest concentrations of trace elements such as V, Sc, Ti, and Cu (Table 2). The CE waters display the highest concentrations of all trace metals (Fig. 4). The Fe concentration is extremely variable but is very high in all of the spring waters (from 370 μg/L in CC to 125,000 μg/L in CE) compared with the average values of rivers worldwide. Thermal springs GA, RM and CE are characterized by the presence of Fe(Mn) oxyhydroxide deposits around the spring orifices. All of the samples generally displayed a decrease in trace metal concentrations with distance from the dome summit (Fig. 4 and Fig. 1).

3.2. Zn concentration and isotope composition in thermal waters

The dissolved Zn concentrations in the thermal springs vary from 1 to 33 μg/L (Table 2) with a mean value of 10 μg/L and a median value of 9 μg/L. These values are similar to or lower than the mean Zn concentrations of thermal waters of other volcanic systems (Aiuppa et al., 2000a,b; Taran et al., 2003; Bortnikova et al., 2009a,b; Kaasalainen and Stefánsson, 2012) but are much higher than the average value (0.6 μg/L) of rivers worldwide (Gaillardet et al., 2005). Therefore, the thermal springs from La Soufrière are enriched in Zn 10 to 200 times compared with the surface waters. The mean Zn concentrations increase towards the summit of the lava dome, with the lowest value (1.6 μg/L) observed in the BCM spring waters and the highest (33 μg/L) observed in the CE waters (Table 2 and Fig. 1). All of the waters have positive correlations between Zn and other trace elements such as Sc and Ti (Fig. 4) as well as Fe and Mn. The Zn concentrations of the thermal waters decrease slightly with temperature (not shown; $y = -0.647x + 36.11$, $r^2 = 0.60$). Except for TA, the Zn concentrations do not display any significant temporal variation during the sampling period. No correlation between Zn concentration and pH is observed. The Bras-David and Capesterre Rivers have concentrations that are comparable

to the mean average Zn concentration of rivers worldwide, confirming that these rivers are not significantly influenced by hydrothermal activity (Lloret et al., 2011; Gaillardet et al., 2011b). The fumarolic gases (condensed solutions) have the highest mean Zn concentrations (128 μg/L) (Table 2).

A summary of the isotopic compositions of Zn in all of the samples is given in Fig. 5. The δ^{66}Zn values in the thermal waters vary from −0.43‰ (BCM) to +1.01‰ (TA-3 was collected in March 2011) with an average value of +0.52‰ (Table 2). This mean value is higher than the δ^{66}Zn values measured in this study for all of the fresh and altered bedrock samples (from −0.14‰ to +0.42‰; Table 2) and the typical δ^{66}Zn value of +0.26‰ that was reported for andesite and basalt (Toutain et al., 2008; Chen et al., 2009a). These results demonstrate that the thermal spring waters are generally enriched in heavier Zn isotopes compared with the host bedrocks. Although all of the spring samples were collected within 4 km of the dome, they display a large δ^{66}Zn variation of 1.44‰, which is 70% of the total δ^{66}Zn range reported in previous studies for hydrothermal systems worldwide (from −0.43‰ to +1.68‰) (Mason et al., 2005; Wilkinson et al., 2005; John et al., 2008; Toutain et al., 2008). No significant temporal variation of Zn isotope compositions is observed except in the TA and GA spring waters (temporal δ^{66}Zn variations of 1.15‰ and 0.26‰, respectively). The Zn isotope composition of the thermal springs does not correlate with pH or temperature. However, a correlation between the mean δ^{66}Zn value and Zn concentration of each spring is observed, with both variables increasing towards the dome's summit (Fig. 6). Similar relationships also exist for δ^{66}Zn vs. Cu, Ti, Mn, Fe and Sc. When the thermal springs with Zn concentrations lower than 5 μg/L are excluded (i.e., CC, TA and BCM), a good correlation is observed between δ^{66}Zn and the ionic strength of solution (Fig. 7). The river waters and fumarolic gas have relatively constant Zn isotope compositions, with mean δ^{66}Zn values of +0.29‰ ± 0.01 and +0.30‰ ± 0.09, respectively (Table 2); these are similar to the values of andesitic bedrock.

The higher δ^{66}Zn values in the thermal springs from Guadeloupe Island indicate that in contrast to riverine inputs (Pons et al., 2013), continental thermal waters are a significant source of heavy Zn isotopes to the ocean.

3.3. Zn concentration and isotope composition in fresh and altered rocks

The Zn concentrations in all of the rocks vary from 12 to 48 μg/g with an average value of 30 μg/g (Table 3). The fresh andesite sample E1215 and the less-altered rock samples 23CF and 31S have higher Zn concentrations than the altered bedrock samples 71S, R805 and R825. The two Fe-precipitation samples have similar but relatively low Zn concentrations (12 and 14 μg/g). The δ^{66}Zn values of all of the rock samples vary from −0.14‰ (R825) to +0.54‰ (pyrite) with an average value of +0.22‰. Interestingly, these values

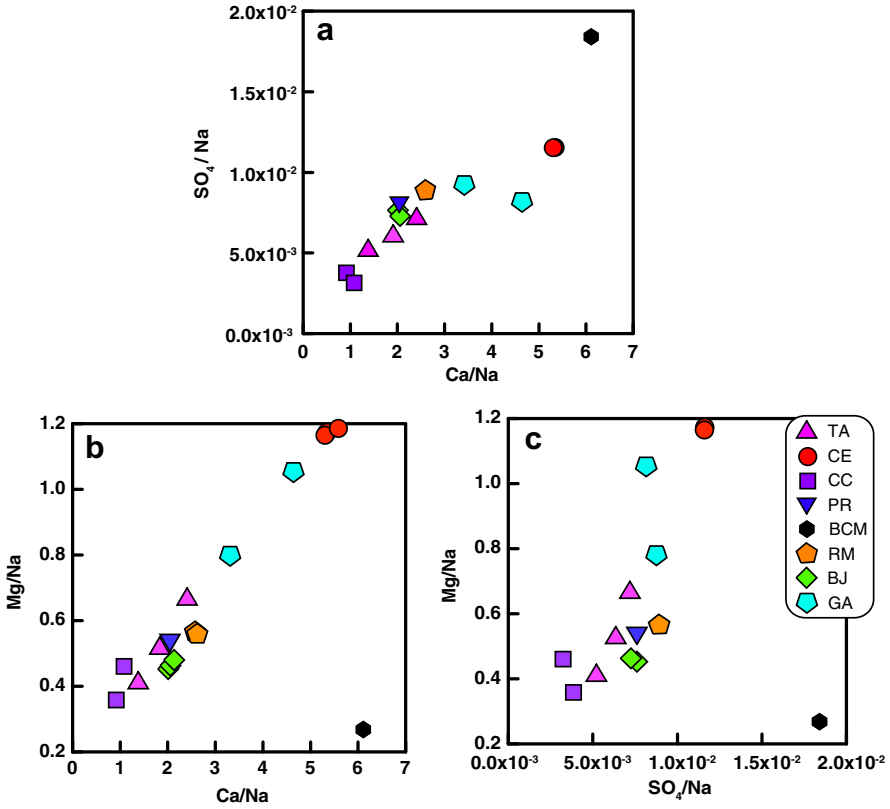

Fig. 3. The geochemical compositions of thermal spring waters in this study. The linear relationships in all of the diagrams may suggest a common geochemical background for these springs. The aberrations of BCM from the linear relationships defined by the other springs in (b) and (c) may be controlled by a different geochemical system.

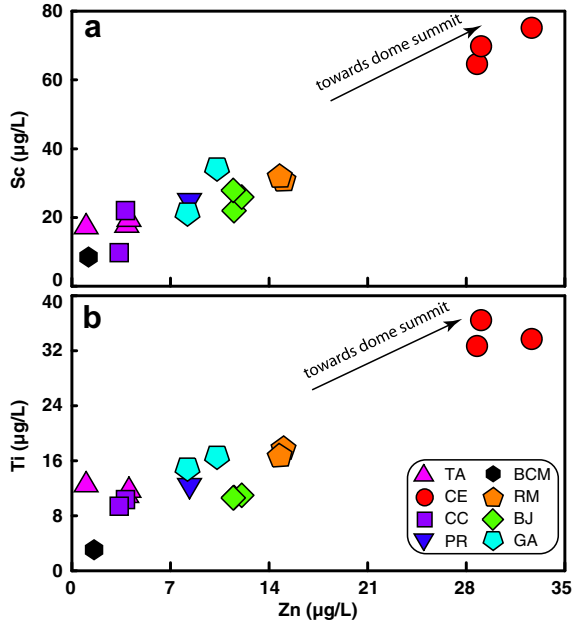

Fig. 4. The correlation between Zn and Sc (a) and Ti (b). Similar relationships can also be observed between the Zn, Cu, Ni, Fe, and Mn concentrations. Because Ti is a refractory element during volcanic degassing, the correlation between Zn and Ti suggests a limited contribution of magmatic gas to Zn in the thermal waters.

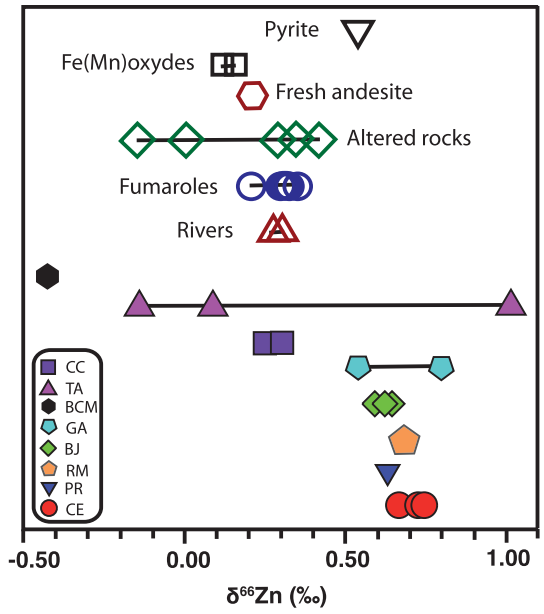

Fig. 5. Systematics of Zn isotopic compositions in different samples from the La Soufrière volcano system analyzed in this study. The dissolved Zn in the spring waters is generally enriched in heavy isotopes compared with the bedrock, whereas hydrothermally altered rocks are depleted in the heavy isotopes.

are generally lower than those of the spring waters (average +0.52‰; Fig. 5 and Table 2). The fresh andesite has a δ^{66}Zn value of +0.21‰, which is similar to the average value of +0.26‰ reported previously for non-altered andesites and basalts (Chapman et al., 2006; Chen et al., 2008, 2009a; Toutain et al., 2008). Compared with the altered rock samples 71S, R805 and R825 (−0.14‰ to +0.29‰), the non-altered or less altered bedrock samples E1215, 23CF and 31S have relatively higher δ^{66}Zn values (+0.21‰ to +0.42‰; Table 3). The two Fe precipitation samples have similar δ^{66}Zn values (+0.12‰ and +0.16‰).

4. DISCUSSION

La Soufrière volcano is located in the Basse-Terre National Park; therefore, anthropogenic pollution is unlikely to be a source of Zn. Rainwater can also be excluded as a source of Zn because the concentration of Zn in remote marine precipitation (approximately 0.29 μg/L; see Halstead et al. (2000) and references therein) is too low to explain the relatively high concentrations observed in the fumarolic gas samples (average 128 μg/L) and in the spring waters (average 10 μg/L; Table 2). Therefore, given the geological context of La Soufrière volcano, magmatic gas and water–rock interactions are the most likely factors that control the Zn concentration and isotopic composition of these fumarolic gases and thermal waters.

4.1. Fumarolic gases

Zn behaves as a volatile element like halogens and other transition metals during magma degassing (Lambert et al., 1988; Allard et al., 1998; Gauthier and Le Cloarec, 1998; Brombach et al., 2000). The magmatic gas, which contains volatile Zn species, may thus be a contributor of Zn to fumarolic gas, as was demonstrated by Toutain et al. (2008) at Merapi volcano. Brombach et al. (2000) showed that fumarolic gas forms at a temperature of approximately 300 °C below the La Soufrière volcano dome and is mainly composed of subsurface water vapors (from an aquifer or infiltration) and components derived from deep magma degassing (e.g., CO_2, H_2S, SO_2 and rare gases; Lambert et al., 1988; Allard et al., 1998; Ruzié et al., 2012). Considering the Mg in the fumarole samples as a refractory element and following the method of Toutain et al. (2008), we calculated that compared with Mg, Zn in the La Soufrière fumaroles is enriched 100 to 8000 times with respect to the bedrock (Tables 2 and 3). These enrichment factors are generally higher than those determined at Merapi (average of 286-fold enrichment), although the fumarole temperature is much lower on Guadeloupe Island (approximately 100 °C) than at Merapi (300–600 °C). These results suggest that magmatic gas is the dominant source of gaseous Zn in fumaroles and that at temperatures between 300 and 100 °C, Zn is not massively scavenged by precipitation of sulfide minerals during its ascent.

Because the geological setting of La Soufrière volcano is very similar to that at Merapi, the processes identified by Toutain et al. (2008) are likely to control the isotopic composition of gaseous Zn in La Soufrière volcano. According to these authors, gaseous Zn derived from magma degassing in the deepest part of Merapi volcano is mainly in the form of $ZnCl_2$(g) (Charlot, 1969; Symonds and Reed, 1993) and has similar or slightly lower δ^{66}Zn values than

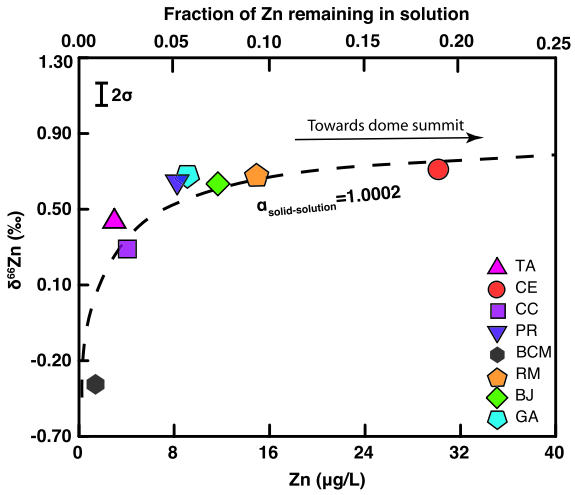

Fig. 6. The correlation between Zn concentration and mean $\delta^{66}Zn$ value in the thermal springs of La Soufrière volcano. The dashed line indicates a Rayleigh adsorption and/or co-precipitation model that shows the magnitude of isotope fractionation induced by Zn adsorption and/or incorporation on solids. The upper *X*-axis is the fraction of Zn remaining in solution (see detailed discussion in the text). The error bars are typical 2 standard deviations of $\delta^{66}Zn$ in the samples of each thermal spring.

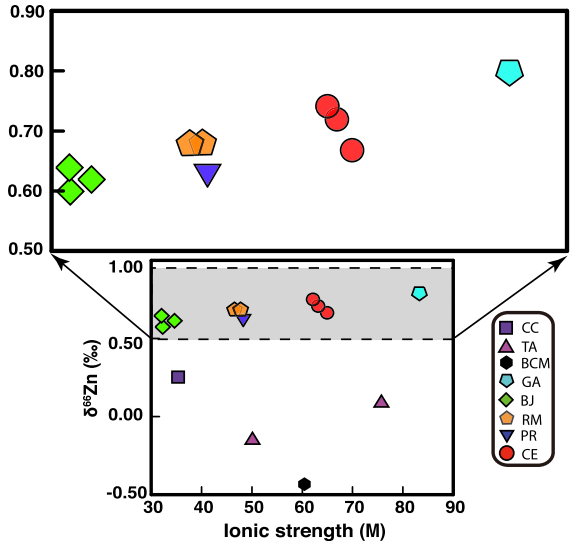

Fig. 7. Relationship between $\delta^{66}Zn$ and the ionic strength of the thermal spring waters. A good correlation is observed when samples with Zn concentrations lower than 5 μg/L are excluded (upper figure), which probably indicates isotopic fractionation associated with the speciation of Zn in solution.

the host andesitic rock. Condensation (and precipitation) of sulfide minerals (i.e., ZnS(s)) then occurs, accompanied by a kinetic isotopic fractionation that increases the gaseous $\delta^{66}Zn$ values during magmatic gas ascent in the volcanic conduits and decreases the Zn concentration (Symonds and Reed, 1993; Mason et al., 2005; Wilkinson et al., 2005; John et al., 2008; Toutain et al., 2008). The overall reaction of gas condensation at temperatures higher than 600 °C can be expressed as:

$$ZnCl_2(g) + H_2S(g) = ZnS(s) + 2HCl(g) \quad (2)$$

Toutain et al. (2008) suggested that when the temperature drops below 600 °C, the Zn isotopes are fractionated by gas condensation at a quasi-isotopic equilibrium, and the solids become enriched in the heavy isotopes. A large decrease of $\delta^{66}Zn$ values of the gaseous phase from +0.85‰ at 600 °C to +0.10‰ at 300 °C was reported by Toutain et al. (2008) at Merapi volcano along with decreasing Zn concentrations. The isotopic composition of the fumarolic gas can be modeled using:

$$\delta^{66}Zn_{gas} = (1000 + \delta^{66}Zn_{gas,0}) \times f^{(\alpha-1)} - 1000 \quad (3)$$

where f represents the remaining Zn fraction in the fumarolic gas phase compared to the initial Zn concentration (at 600 °C), α is the isotopic fractionation factor between the solid and the vapor, and $\delta^{66}Zn_{gas,0}$ is the isotopic composition of the initial fumarolic gas before condensation. According to the temperature dependency of α proposed by Toutain et al. (2008), the equilibrium fractionation factor should be approximately 1.0035 at 100 °C and 1.0015 at 300 °C. Taking a value of +0.85‰ for $\delta^{66}Zn_{gas,0}$ as proposed by Toutain et al. (2008) for Merapi, we calculated that the remaining gaseous Zn fraction f should be between 0.8 and 0.9 to account for the relatively constant $\delta^{66}Zn$ value of +0.30‰ measured in the La Soufrière fumaroles at 100 °C. The same calculation indicates that $f = 0.7$ at 300 °C. This sensitivity test indicates that the values of $\delta^{66}Zn_{gas}$ measured in the La Soufrière fumaroles can be explained using the fumarolic gas emission model of Toutain et al. (2008) and that the proportion of Zn condensed into the solid phase has to be relatively small at temperatures below 300 °C.

Accordingly, the final magmatic gas would have $\delta^{66}Zn$ values between +0.80‰ and +0.30‰, which is compatible with the Zn isotopic composition of the thermal waters (Table 2). If gaseous Zn derived from magma degassing were a source of the dissolved Zn found in the spring waters, the relationship between $\delta^{66}Zn$ and Zn concentration (Fig. 6) would reflect variable contributions of magmatic gas to the aquifers. In this case, lower concentrations and $\delta^{66}Zn$ values would correspond to the dissolution of magmatic gas at relatively low temperatures (large proportion of condensed Zn during gas ascent), while higher Zn concentrations and $\delta^{66}Zn$ values would imply the dissolution of Zn derived from hot gas. This scenario, however, is not consistent with either the decrease of Zn concentration with increasing temperature observed in this study (Table 2) or with the good correlation observed in the thermal springs between the dissolved Ti and Zn concentrations (Fig. 4b) because Ti is a refractory element in magmatic gas (Aiuppa et al., 2000a,b; Toutain et al., 2008). Therefore, although the model of magmatic Zn degassing can explain the isotopic composition of Zn in the fumaroles, it remains unlikely that magmatic gas contributes to the dissolved Zn in the thermal springs at La Soufrière volcano. The zinc concentrations and isotope abundances in the fumaroles are likely decoupled from those of the thermal springs.

Table 3
Zn isotopic composition and elemental concentrations in bedrock materials of La Soufrière volcano, Guadeloupe (n, number of Zn isotopic measurements; AI(Zn), alteration index of rocks; Zn isotope analytical uncertainties are 2 external standard deviations (2σ)).

ID	n	Sample	δ^{66}Zn (‰)	AI(Zn)	Na (μg/g)	Mg (μg/g)	Ti (μg/g)	Fe (μg/g)	Ni (μg/g)	Cu (μg/g)	Zn (μg/g)	Zr (μg/g)	Sn (μg/g)
E1215	5	Fresh andesite	0.21 ± 0.05	1.1	19800	25,000	4520	58,000	15	60	41	80	1
23CF	3	Less-altered rock	0.42 ± 0.07	0.9	19400	26,500	4560	59,800	16	75	48	77	1
31S	5	Intermediately-altered rock	0.35 ± 0.05	1.5	2620	16,800	7100	24,200	4	8	43	115	1
71S	5	Altered rock	0.29 ± 0.08	1.3	3060	10,400	6820	13,000	4	15	35	84	2
R805	4	Altered rock	0.01 ± 0.07	2.0			6170	67,700	2	91	26	95	4
R825	4	Altered rock	-0.14 ± 0.03	2.2			5450	56,700	3	52	24	93	4
GA-M	3	Fe-precipitation	0.12 ± 0.01				25	522,000		7	12		
GA-S	3	Fe-precipitation	0.16 ± 0.03				120	502,000		12	14		
Pyrite	3	Pyrite mineral	0.54 ± 0.04										

4.2. Thermal spring waters

4.2.1. Main contribution from water–rock interactions

Zinc is known to be a soluble element that is present in both dissolved and particulate loads in surface water (Möller and Giese, 1997; Bau et al., 1998; Metz and Trefry, 2000; Chen et al., 2008). In this study, the behavior of Zn during water–rock interactions at high temperatures was first investigated based on the suite of rock samples with different degrees of hydrothermal alteration. To evaluate the mobility of Zn, a Zn alteration index (AI(Zn)) for each rock sample was defined using Zr as an immobile element during water–rock interaction (Aiuppa et al., 2000b):

$$\mathrm{AI(Zn)} = (\mathrm{Zr/Zn})_a/(\mathrm{Zr/Zn})_0 \quad (4)$$

where $(Zr/Zn)_a$ and $(Zr/Zn)_0$ represent the concentration ratios of Zr to Zn in altered rocks and in unaltered fresh andesite, respectively. The calculated AI(Zn) values vary from 0.9 for less-altered rock (23CF) to 2.2 for the most-altered rock (R825; Table 3). The high AI(Zn) values (>1) indicate that Zn is mobile compared to Zr. Because Na is known to be the most mobile element during water–rock interactions, we also calculated the alteration index for Na (AI(Na)) using the Zr/Na concentration ratios instead of Zr/Zn in Eq. (4). The results indicate that even though Na cannot be measured in the most-altered rocks (R805, R825), the defined AI(Na) values increase up to 7 in the altered samples (71S, 31S). This finding indicates that Zn is less mobile than Na during the water–rock interactions or that Zn is retained in the secondary precipitate phases after dissolution.

The relative mobility of Zn during water–rock interactions can also be estimated by comparing Na with Zn in the dissolved phase in the thermal springs. Following Aiuppa et al. (2000a,b), we can calculate the enrichment factor of Zn (EF(Zn)) in the spring waters with:

$$\mathrm{EF(Zn)} = (\mathrm{Zn/Na})_w/(\mathrm{Zn/Na})_0 \quad (5)$$

where $(Zn/Na)_w$ and $(Zn/Na)_0$ represent the concentration ratios of Zn to Na dissolved in the thermal water and in the fresh andesite, respectively. Like Mg, Na is a non-volatile element during magma degassing (Aiuppa et al., 2000a,b) and is essentially derived from rock dissolution. Given the intensity of hydrothermal alteration, we assume that the magmatic and atmospheric contributions for Na are limited in the thermal waters (Losno et al., 1991; Aiuppa et al., 2000a). Considering the mean concentrations of 40 μg/g for Zn and 2.03% for Na in the local host andesite (Table 3 and Boudon et al., 2008), the calculated EF(Zn) values vary from 0.01 to 0.25 in all of the spring waters with an average value of 0.08. These numbers, which are deduced from the dissolved load, confirm that Zn is less mobile than Na in the hydrothermal system, as indicated by the discussion about the solids presented above. Therefore, processes that reincorporate Zn that has dissolved from rocks must occur in hydrothermal systems. If sources other than the parent bedrock contribute to the dissolved Zn, this conclusion would even be more robust.

All of the altered and non-altered rocks have δ^{66}Zn values between −0.14‰ and +0.42‰ (Table 3 and Fig. 5). Fresh andesite (E1215) has a δ^{66}Zn value of +0.21‰, which is consistent with the reported average δ^{66}Zn value of +0.26‰ for non-altered andesites and basalts and is slightly lower than the mean integrated value of +0.30‰ for terrestrial silicates (Chapman et al., 2006; Chen et al., 2008, 2009a; Toutain et al., 2008; Pons et al., 2013). Table 3 and Fig. 8 show that the more intense the loss of Zn from the rock, the lower the δ^{66}Zn value for altered rocks, with the most-altered samples exhibiting values close to or lower than 0.00‰ (i.e., R825). These results suggest that water–rock interaction fractionates the Zn isotopes and that heavy Zn isotopes (e.g. ^{66}Zn) are preferentially released into solution during hydrothermal alteration.

Based on the discussion presented above, the mass balance of Zn between the fresh andesite and the altered rock and the solution can be expressed as follows:

$$M_0[\mathrm{Zn}]_0 = M_a[\mathrm{Zn}]_a + M_w[\mathrm{Zn}]_w \quad (6)$$

where *0*, a and w denote the fresh andesite, altered rock and solution, respectively, M is the mass of the rocks (both fresh and altered) or the reacting solution, and [Zn] refers to the Zn concentration. We can also calculate the isotopic composition of Zn ($\delta^{66}Zn_w$) released via water–rock interaction into solution using:

$$M_0[\mathrm{Zn}]_0\delta^{66}\mathrm{Zn}_0 = M_a[\mathrm{Zn}]_a\delta^{66}\mathrm{Zn}_a + M_w[\mathrm{Zn}]_w\delta^{66}\mathrm{Zn}_w \quad (7)$$

For the insoluble element Zr, the concentration in solution is very low, and the Zr mass balance can thus be calculated as:

$$M_0[\mathrm{Zr}]_0 = M_a[\mathrm{Zr}]_a \quad (8)$$

By combining Eqs. (4), (6), (7), and (8), the isotopic composition of Zn in solution can be calculated as:

$$\delta^{66}\mathrm{Zn}_w = \frac{\mathrm{AI(Zn)}\delta^{66}\mathrm{Zn}_0 - \delta^{66}\mathrm{Zn}_a}{\mathrm{AI(Zn)} - 1} \quad (9)$$

Taking the values of the unaltered materials (E1215, 23CF) and of the most-altered rock (R825), the final $\delta^{66}Zn_w$ value is calculated to be approximately +0.70‰ for Zn released into solution. Calculations using insoluble elements such as Ti, Th and REEs provided similar results. The value of +0.70‰ is similar to the observed higher δ^{66}Zn values in most of the thermal springs (i.e., CE, TA, and GA). This simple calculation suggests that to first order, water–rock interaction is a possible source of Zn in thermal spring waters and that Zn is partly mobile.

Similarly, the enrichment factor of Zn in solution that is derived from water–rock interaction can be predicted by introducing a similar mass budget equation of (6) for Na:

$$\mathrm{EF(Zn)} = \frac{1 - \mathrm{AI(Zn)}^{-1}}{1 - \mathrm{AI(Na)}^{-1}} \quad (10)$$

This calculation predicts EF(Zn) values of 0.4–0.5 depending on the Na concentrations in the host rocks, which are higher than those measured in the thermal waters (from 0.01 to 0.25). These values indicate that less Zn was measured in the spring waters compared with what is expected based on the mass budget calculation despite the fact that water–rock interaction can potentially explain the range of δ^{66}Zn variability in the thermal waters of Guadeloupe Island. Therefore, we conclude that if water–rock interaction is the dominant process that provides Zn to thermal waters, scavenging processes must exist to remove Zn from solution.

4.2.2. Possible mechanisms of fractionating Zn isotopes during water–rock interaction

The discussion presented above shows that Zn isotopes are probably fractionated during high temperature alteration due to the incorporation of Zn into secondary insoluble compounds such as sulfides, oxyhydroxides, carbonates, phosphates, clay minerals (Bau et al., 1998; Aiuppa et al., 2000a,b) or organic compounds. In this study, it was not possible to perform precise calculations of Zn speciation in thermal waters due to the lack of redox and H_2S concentration data. In addition, the composition of the solution that is interacting with host rocks at high temperatures is difficult to constrain. We can only qualitatively suggest the possible mechanisms that are responsible for the observed Zn isotope fractionation. The *ab initio* calculations recently performed by Black et al. (2011), Fujii et al. (2011) and Fujii and Albarède (2012) predicted that in relatively low-pH, SO_4-rich solutions such as the La Soufrière thermal waters, Zn sulfide species are enriched in light isotopes compared to Zn sulfate, carbonate and chloride species. Therefore, the preferential precipitation of Zn sulfide (in the form of sphalerite) would increase

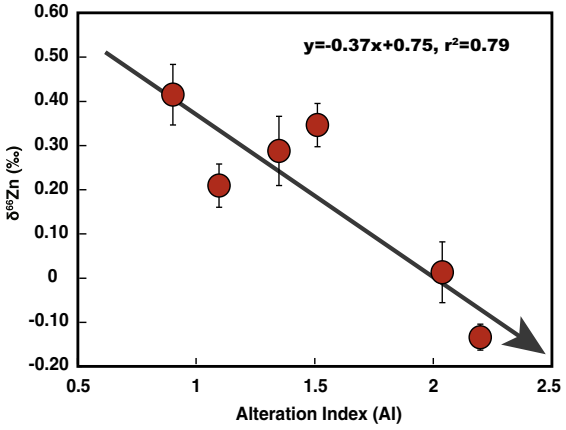

Fig. 8. Relationship between δ^{66}Zn and the alteration index AI(Zn) for bedrocks (points). AI(Zn) is defined as the concentration ratio of Zr/Zn in an individual bedrock sample to that of unaltered bedrock (1215E and 23CF; see text for detail). The decrease of δ^{66}Zn with increasing AI(Zn) value (degree of alteration) implies the preferential release of heavier Zn isotopes (^{66}Zn) into solution during water–rock interactions at relatively high temperatures.

the δ^{66}Zn values of the solution. John et al. (2008) showed that in seafloor hydrothermal vents, the precipitation of sulfide (sphalerite) leads to the enrichment of heavy isotopes in the solution (up to 1‰). Other studies have also reported that sulfides from volcanic chimneys, as well as sulfide deposits from various hydrothermal settings, are isotopically light (Mason et al., 2005; Wilkinson et al., 2005; John et al., 2008; Toutain et al., 2008). These results confirm that the precipitation of Zn sulfides is a reasonable mechanism for depleting solutions of light isotopes during water–rock interactions. The correlation between Zn isotopic composition and ionic strength in most thermal springs confirms that the enrichment of heavy Zn isotopes (e.g., ^{66}Zn) in the thermal springs is related to Zn speciation in the solution (Fig. 7).

The extraction of organic-bound Zn from the solution is another possible mechanism (Gelabert et al., 2006; John et al., 2007; Fujii and Albarède, 2012). However, given the relatively high temperatures of the La Soufrière thermal waters, this process is probably less plausible. Finally, the altered rocks with low δ^{66}Zn values in this study (71S, R805, R825) are enriched in clay minerals, so we cannot exclude the possible incorporation of Zn into hydrothermal clay minerals that could fractionate the Zn isotopes and favor the light isotopes. To our knowledge, no study has reported Zn isotope fractionation during the formation of hydrothermal clays. Viers et al. (2007) investigated the Zn isotope compositions of lateritic soils in Cameroon and showed a significant depletion of heavy Zn isotopes in the most weathered superficial horizon (enriched in clay minerals), which indicates possible Zn isotopic fractionation associated with clay formation.

4.2.3. The co-precipitation and adsorption effects

As shown in Fig. 6, low dissolved Zn concentrations in the thermal waters are associated with low δ^{66}Zn values

(+0.32‰, +0.28‰ and −0.43‰ for TA, CC and BCM, respectively). For these samples, the linear relationship between the $\delta^{66}Zn$ values and the solution's ionic strength is no longer observed (Fig. 7). Interestingly, these waters have the highest Na concentrations (Table 2), which suggest very intense water–rock interactions. The most likely mechanism to explain the contrasting behaviors of these Zn-depleted samples is the secondary co-precipitation of Zn into Fe oxyhydroxides and/or Zn adsorption. Previous experimental studies have shown that these processes generally favor heavy Zn isotopes in solids (Pokrovsky et al., 2005; Balistrieri et al., 2008; Juillot et al., 2008). The results of these experiments are consistent with the enrichment of heavy Zn isotopes (e.g., ^{66}Zn) found in oceanic Fe-Mn oxides (Marechal et al., 2000) and in soil iron nodules (Viers et al., 2007).

To test this hypothesis, we calculated the Zn isotopic fractionation and $\delta^{66}Zn$ values in solution ($\delta^{66}Zn_{sol}$) using a simple Rayleigh model:

$$\delta^{66}Zn_{sol} = (\delta^{66}Zn_0 + 1000) \times f^{(\alpha-1)} - 1000 \quad (11)$$

where $\delta^{66}Zn_0$ refers to the Zn isotope composition in the initial solution, and α and f are the solid-solution fractionation factor and the fraction of Zn remaining in solution, respectively. Assuming that the initial solution has the same Na concentration as the thermal spring waters, the initial concentration of Zn in solution was calculated to be approximately 100–130 μg/L using Eq. (10). Considering +0.70‰ for the initial $\delta^{66}Zn_0$ value (see the discussion above), the isotopic composition of the Zn remaining in solution can thus be calculated and is illustrated in Fig. 6 (dashed line). The $\delta^{66}Zn$ values of the Zn-depleted spring waters (BCM, CC and TA) can be explained by choosing a fractionation factor α of 1.0002, which is an average value reported in previous experimental studies (Pokrovsky et al., 2005; Gelabert et al., 2006; John et al., 2007; Balistrieri et al., 2008; Juillot et al., 2008). This calculation suggests that co-precipitation and adsorption are possible processes that scavenge Zn from solution after the water–rock interaction. For example, the results indicate that for the BCM spring, more than 95% of the Zn has been scavenged.

While the adsorption or co-precipitation of Zn onto solids is a reasonable mechanism to explain the lower $\delta^{66}Zn$ values found in the TA, CC and BCM springs, the two Fe precipitates at the orifice of the GA springs have relatively low values (+0.12‰ and +0.16‰, Fig. 5) compared to the mean value of +0.67‰ for dissolved Zn (Table 2). We suggest that kinetic fractionation (preferential incorporation of light isotopes), temperature effects or the incorporation of trace sulfides in the solid can explain the enrichment of light isotopes in Fe oxyhydroxides. If the explanation of Fe-oxide precipitation holds, the Zn isotope data show that it should not affect all of the springs of La Soufrière's dome, due to the diversity of hydrological conditions and the complexity of the volcanic conduits. This may explain the temporal $\delta^{66}Zn$ variation from +1.01‰ in the spring to −0.14‰ in the autumn in the TA spring. More work is thus needed to decipher the Zn isotopic fractionation during hydrothermal Fe mineral formation.

4.3. Low temperature water–rock interaction processes

The surface waters of the Capesterre and Bras-David Rivers have relatively low EF(Zn) values (0.01 and 0.02, respectively). Because these rivers are located far from the active volcanic region and are entirely controlled by soil weathering processes (Lloret et al., 2011; Gaillardet et al., 2011b), the low EF(Zn) values reflect the limited Zn mobility at surface temperatures. Moreover, the two river samples have identical $\delta^{66}Zn$ values of +0.28‰, which is similar to the average $\delta^{66}Zn$ value of +0.26‰ for the host andesites of Guadeloupe Island. These results indicate that little Zn isotope fractionation occurs during surface soil weathering, in contrast with the water–rock interaction in the hydrothermal systems. Although more work is needed to investigate the Zn isotopic variations during rock weathering under surface conditions, our data suggest that Zn isotopes likely fractionate differently during water–rock interactions at high temperatures, especially in active volcanic systems. The high ionic strength at high temperatures may favor the formation of aqueous complexes with variable Zn isotopic compositions (Fujii et al., 2011). The adsorption or co-precipitation of Zn will therefore induce isotopic variations if the different complexes do not have the same affinity for surfaces. At low temperatures, this competition between aqueous and surface Zn species might be less important. An alternative explanation is that the competing effects of variable fractionation lead to no apparent isotopic variation in soils during low temperature chemical weathering, as was demonstrated by Viers et al. (2007) in the saprolite soil horizon. Clearly, the behavior of Zn isotopes in soils and watersheds in different weathering regimes requires more work.

5. CONCLUSIONS

We developed a purification method that allowed us to accurately measure the Zn isotopic ratios of waters from eight thermal springs on the summit dome of the active La Soufrière volcano. Although higher Zn concentrations are observed in all of the thermal waters compared with rivers worldwide, the spring samples are depleted in Zn with respect to the very mobile element Na. The most important observation of this study is that the spring waters are generally enriched in heavier Zn isotopes (i.e., ^{66}Zn) relative to the host bedrocks. This indicates that unlike continental riverine inputs, the contribution of thermal waters to the ocean is characterized by the enrichment of heavy Zn isotopes. All of the spring water samples collected in a 4-km radius around the dome have a large $\delta^{66}Zn$ variation of 1.44‰ and increased $\delta^{66}Zn$ values with Zn concentration towards the dome's summit. Although Zn is a volatile element and a magmatic degassing model can explain the Zn concentrations and isotopic composition of the fumaroles, our data indicate that water–rock interaction is the main contribution of Zn in thermal springs. A mass budget calculation based on a suite of andesites with varying degrees of alteration indicates that Zn is mobile and that heavier Zn isotopes are preferentially released into solution during water–rock interactions at relatively high temperatures.

However, the dissolved Zn concentrations predicted by this mass budget approach are higher than those measured in the spring waters, which indicates the existence of a secondary sink of Zn in the hydrothermal systems. This can most likely be explained by Zn co-precipitation during the formation of Fe(Mn) oxide-hydroxides and Zn adsorption. Given the economic value of Zn, more work is clearly needed to investigate the scavenging of Zn in volcanic systems that is induced by precipitation, adsorption or condensation. The results of this preliminary study highlight the potential of Zn isotopes to trace water–rock interaction processes and metal behaviors in hydrothermal zones.

ACKNOWLEDGMENTS

This work benefited from the logistical support of OVSG. The authors thank J. Bouchez, T. Bullen, P. Allard and F. Albarède for their constructive discussions and J. Moureau for analytical assistance. Thanks are extended to associate editor M. Rehkämper and reviewers J. Sonke, N. Mattielli and S. Nielsen for their thorough and insightful comments on the first version of the manuscript. The authors acknowledge associate editor Jeff Alt, reviewers J. Sonke and R. Wanty and the anonymous referee who greatly improved the quality of the manuscript. J.-B. Chen was financially supported by an IPGP ATER fellowship and the "Hundred Talents" project of the Chinese Academy of Sciences. This is IPGP contribution No. 3468.

REFERENCES

Aiuppa A., Allard P., D'Alessandro W., Michel A., Parello F., Treuil M. and Valenza M. (2000a) Mobility and fluxes of major, minor and trace metals during basalt weathering and groundwater transport at Mt. Etna volcano (Sicily). *Geochim. Cosmochim. Acta* **64**(11), 1827–1841.

Aiuppa A., Dongarrà G., Capasso G. and Allard P. (2000b) Trace elements in the thermal groundwaters of Vulcano Island (Sicily). *J. Volcanol. Geoth. Res.* **98**(1–4), 189–207.

Allard P., Hammouya G. and Parello F. (1998) Dégazage magmatique diffus a la Soufrière de Guadeloupe, Antilles. *C. R. Acad. Sci. Paris IIA* **327**, 315–318.

Archer C. and Vance D. (2004) Mass discrimination correction in multiple-collector plasma source mass spectrometry, an example using Cu and Zn isotopes. *J. Anal. At. Spectrom.* **19**, 656–665.

Balistrieri L. S., Borrok D. M., Wanty R. B. and Ridley W. I. (2008) Fractionation of Cu and Zn isotopes during adsorption onto amorphous Fe(III) oxyhydroxide: experimental mixing of acid rock drainage and ambient river water. *Geochim. Cosmochim. Acta* **72**(2), 311–328.

Bau M., Usui A., Pracejus B., Mita N., Kanai Y., Irber W. and Dulski P. (1998) Geochemistry of low-temperature water–rock interaction, evidence from natural waters, andesite, and iron-oxyhydroxide precipitates at Nishiki-numa iron-spring, Hokkaido, Japan. *Chem. Geol.* **151**(1–4), 293–307.

Bernard M.-L., Molinie J., Petit R.-H., Beauducel F., Hammouya G. and Marion G. (2006) Remote and in situ plume measurements of acid gas release from La Soufrière volcano, Guadeloupe. *J. Volcanol. Geoth. Res.* **150**, 395–409.

Bigot S., Boudon G., Semet M. and Hammouya G. (1994) Traçage chimique de la circulation des eaux souterraines sur le volcan de la Grande Découverte (La Soufrière), Guadeloupe. *C. R. Acad. Sci. IIA* **318**, 1215–1221.

Bigot S. and Hammouya G. (1987) Surveillance hydrogéochimique de la Soufrière de Guadeloupe, 1979–1985, diminution de l'activité ou confinement? *Acad. Sci. Paris* **304**, 757–760.

Black R. J., Kavner A. and Schauble A. E. (2011) Calculation of equilibrium stable isotope partition function ratios for aqueous zinc complexes and metallic zinc. *Geochim. Cosmochim. Acta* **75**, 769–783.

Borrok D. M. et al. (2007) Separation of copper, iron, and zinc from complex aqueous solutions for isotopic measurement. *Chem. Geol.* **242**(3–4), 400–414.

Bortnikova S. B., Bessonova E. P. and Trofimova E. P., et al. (2009a) The hydrology and geochemistry of gas-hydrothermal springs on Ebeko volcano, Paramushir I. *Vulkanol. Seismol.* **1**, 39–51.

Bortnikova S. B., Gavrilenko G. M., Bessonova E. P. and Lapukhov A. S. (2009b) The hydrogeochemistry of thermal springs on Mutnovskii volcano, southern Kamchatka. *J. Volcanol. Seismolog.* **3**(6), 388–404.

Boudon G., Komorowski J.-C., Villemant B. and Semet M. P. (2008) A new scenario for the last magmatic eruption of La Soufrière of Guadeloupe (Lesser Antilles) in 1530 A.D. Evidence from stratigraphy radiocarbon dating and magmatic evolution of erupted products. *J. Volcanol. Geoth. Res.* **178**(3), 474–490.

Brombach T., Marini L. and Hunziker J. C. (2000) Geochemistry of the thermal springs and fumaroles of Basse-Terre Island, Guadeloupe, Lesser Antilles. *Bull. Volcanol.* **61**(7), 477–490.

Caliro S., Chiodini G., Avino R., Cardellini C. and Frondini F. (2005) Volcanic degassing at Somma-Vesuvio (Italy) inferred by chemical and isotopic signatures of groundwater. *Appl. Geochem.* **20**(6), 1060–1076.

Chapman J. B., Mason T. F. D., Weiss D. J., Coles B. J. and Wilinson J. J. (2006) Chemical separation and isotopic variations of Cu and Zn from five geological reference materials. *Geostand. Geoanal. Res.* **30**, 5–16.

Charlot G. (1969) *Les réactions chimiques en solution, l'analyse qualitative minérale*. Masson & Cie Paris, p. 286–288.

Chen J. -B. (2008) La contamination métallique de la Seine et des rivières de son bassin, traçage par les isotopes du zinc. PhD thesis, Institut de Physoque du Globe de Paris. 202p.

Chen J.-B., Gaillardet J. and Louvat P. (2008) Zinc isotopes in the Seine River water, France, a probe of anthropogenic contamination. *Environ. Sci. Technol.* **40**, 6494–6501.

Chen J.-B., Gaillardet J., Louvat P. and Huon S. (2009a) Zn isotopes in the suspended load of the Seine River, France, isotopic variations and source determination. *Geochim. Cosmochim. Acta* **73**(14), 4060–4076.

Chen J.-B., Louvat P., Gaillardet J. and Birck J.-L. (2009b) Direct separation of Zn from dilute aqueous solutions for isotope composition determination using multi-collector ICP-MS. *Chem. Geol.* **259**(3–4), 120–130.

Cheynet B., Dall'Aglio M., Garavelli A., Grasso M. F. and Vurro F. (2000) Trace elements from fumaroles at Vulcano Island (Italy), rates of transport and a thermochemical model. *J. Volcanol. Geoth. Res.* **95**(1–4), 273–283.

Chiodini G., Allard P., Caliro S. and Parello F. (2000) ^{18}O exchange between steam and carbon dioxide in volcanic and hydrothermal gases, implications for the source of water. *Geochim. Cosmochim. Acta* **64**(14), 2479–2488.

Cloquet C., Carignan J., Lehmann M. and Vanhaecke F. (2008) Variation in the isotopic composition of zinc in the natural environment and the use of zinc isotopes in biogeosciences: a review. *Anal. Bioanal. Chem.* **390**, 451–463.

Cortecci G., Dinelli E., Bolognesi L., Boschetti T. and Ferrara G. (2001) Chemical and isotopic compositions of water and

dissolved sulfate from shallow wells on Vulcano Island, Aeolian Archipelago, Italy. *Geothermics* **30**(1), 69–91.

Dessert C., Dupré B., Gaillardet J., François L. M. and Allègre C. J. (2003) Basalt weathering laws and the impact of basalt weathering on the global carbon cycle. *Chem. Geol.* **202**(3–4), 257–273.

Dessert C., Gaillardet J., Dupré B., Schott J. and Pokrovsky O. S. (2009) Fluxes of high- versus low-temperature water–rock interactions in aerial volcanic areas, example from the Kamchatka Peninsula, Russia. *Geochim. Cosmochim. Acta* **73**, 148–169.

Feuillard M., Allegre C. J., Brandeis G., Gaulon R., Lemouel J. L., Mercier J. C., Pozzi J. P. and Semet M. P. (1983) The 1975–1977 crisis of La Soufrière de Guadeloupe (FWI)-a still born magmatic eruption. *J. Volcanol. Geoth. Res.* **16**(3–4), 317–334.

Fujii T. and Albarède F. (2012) Ab initio calculation of the Zn isotope effect in phosphates, citrates, and malates and applications to plants and soil. *PLoS ONE* **7**(2), e30726. http://dx.doi.org/10.1371/journal.pone.0030726.

Fujii T., Moynier F., Pons M.-L. and Albarède F. (2011) The origin of Zn isotope fractionation in sulfides. *Geochim. Cosmochim. Acta* **75**, 7632–7643.

Gagnevin D., Boyce A. J., Barrie C. D., Menuge J. F. and Blakeman R. J. (2012) Zn, Fe and S isotope fractionation in a large hydrothermal system. *Geochim. Cosmochim. Acta* **88**, 183–198.

Gaillardet J., Viers J. and Dupré B. (2005) Trace element in river waters. *Treatise on Geochemistry. Surface and Ground Water Weathering and Soils* **vol. 5**, 225–272.

Gaillardet J., Louvat P. and Lajeunesse E. (2011a) Rivers from volcanic island arcs, the subduction weathering factory. *Appl. Geochem.* **26**, S350–S353.

Gaillardet J., Rad S., Rivé K., Louvat P., Gorge C., Allègre C.-J. and Lajeunesse E. (2011b) Orography-driven chemical denudation in the Lesser Antilles, evidence for a new feed-back mechanism stabilizing atmospheric CO_2. *Am. J. Sci.* **311**, 851–894.

Gauthier P.-J. and Le Cloarec M.-F. (1998) Variability of alkali and heavy metal fluxes released by Mt. Etna volcano, Sicily, between 1991 and 1995. *J. Volcanol. Geoth. Res.* **81**, 311–326.

Gelabert A., Pokrovsky O. S., Viers J., Schott J., Boudou A. and Feurtet-Mazel A. (2006) Interaction between zinc and freshwater and marine diatom species, surface complexation and Zn isotope fractionation. *Geochim. Cosmochim. Acta* **70**(4), 839–857.

Halstead J. R. M., Cunninghame G. R. and Hunter K. (2000) Wet deposition of trace metals to a remote site in Fiordland, New Zealand. *Atmos. Environ.* **34**, 665–676.

Hirn A., Michel B. (1979) Evidence of migration of main shocks during major seismo-volcanic crises of La Soufrière (Guadeloupe, Lesser Antilles) in 1976. J. Volcanol. Geoth. Res., 1979. 6(3–4): 295-304.

John S. G., Geis R. W., Saito M. A. and Boyle E. A. (2007) Zinc isotope fractionation during high-affinity and low-affinity zinc transport by the marine diatom *Thalassiosira oceanica*. *Limnol. Oceanogr.* **52**, 2710–2714.

John S. G., Rouxel O. J., Craddock P. R., Engwall A. M. and Boyle E. A. (2008) Zinc stable isotopes in seafloor hydrothermal vent fluids and chimneys. *Earth Planet. Sci. Lett.* **269**(1–2), 17–28.

Joseph E. P., Fournier N., Lindsay J. M. and Fischer T. P. (2011) Gas and water geochemistry of geothermal systems in Dominica, Lesser Antilles island arc. *J. Volcanol. Geoth. Res.* **206**, 1–14.

Juillot F., Marechal C., Ponthieu M., Cacaly C., Morin G., Benedetti M., Hazemann J. L., Proux O. and Guyot F. (2008) Zn isotopic fractionation caused by sorption on goethite and 2-lines ferrihydrite. *Geochim. Cosmochim. Acta* **72**, 4886–4900.

Kaasalainen H. and Stefánsson A. (2012) The chemistry of trace elements in surface geothermal waters and steam, Iceland. *Chem. Geol.* **330–331**, 60–85.

Lambert G., Le Cloarec M.-F. and Pennisi M. (1988) Volcanic output of SO_2 and trace metals, a new approach. *Geochim. Cosmochim. Acta* **52**, 39–42.

Leeman W. P., Tonarini S., Pennisi M. and Ferrara G. (2005) Boron isotopic variations in fumarolic condensates and thermal waters from Vulcano Island, Italy, implications for evolution of volcanic fluids. *Geochim. Cosmochim. Acta* **69**(1), 143–163.

Lloret E., Dessert C., Gaillardet J., Albéric P., Crispi O., Chaduteau C. and Benedetti M. (2011) Comparison of dissolved inorganic and organic carbon yields and fluxes in the watersheds of tropical volcanic islands, examples from Guadeloupe (French West Indies). *Chem. Geol.* **280**, 65–78.

Losno R., Bergametti G., Carlier P. and Mouvier G. (1991) Major ions in marib=ne rainwater with attention to sources of alkaline and acidic species. *Atmos. Environ. A-Gen.* **25**(3–4), 763–770.

Louvat P. and Allègre C. J. (1997) Present denudation rates on the island of RÈunion determined by river geochemistry, basalt weathering and mass budget between chemical and mechanical erosions. *Geochim. Cosmochim. Acta* **61**(17), 3645–3669.

Louvat P., Gaillardet J., Paris G. and Dessert C. (2011) Boron isotope ratios of surface waters in Guadeloupe, Lesser Antilles. *Appl. Geochem.* **26**, S76–S79.

Macdonald R., Hawkesworth C. J. and Heath E. (2000) The Lesser Antilles volcanic chain, a study in arc magmatism. *Earth Sci. Rev.* **49**(1–4), 1–76.

Marechal C., Nicolas E., Douchet C. and Albarede F. (2000) Abundance of zinc isotopes as a marine biogeochemical tracer. *Geochem. Geophys. Geosyst.* **1**. http://dx.doi.org/10.1029/1999GC000029.

Marechal C., Telouk P. and Albarede F. (1999) Precise analysis of copper and zinc isotopic compositions by plasma-source mass spectrometry. *Chem. Geol.* **156**, 251–273.

Mattielli N., Petit J., Deboudt K., Flament P., Perdrix E., Taillez A., Rimetz-Planchon J. and Weis D. (2009) Zn isotope study of atmospheric emissions and dry depositions within a 5 km radius of a Pb–Zn refinery. *Atmos. Environ.* **43**, 1265–1272.

Mason T. F. D., Weiss D., Chapman B. J., Wilkinson J. J., Tessalina G. S., Spiro B., Hortstwood S. A. M., Spratt J. and Coles J. B. (2005) Zn and Cu isotopic variability in the Alexandrinka volcanic-hosted massive sulphide (VHMS) ore deposit, Urals, Russia. *Chem. Geol.* **221**(3–4), 170–187.

Metz S. and Trefry J. H. (2000) Chemical and mineralogical influences on concentrations of trace metals in hydrothermal fluids. *Geochim. Cosmochim. Acta* **64**(13), 2267–2279.

Millot R., Scaillet B. and Sanjuan B. (2010) Lithium isotopes in island arc geothermal systems, Guadeloupe, Martinique (French West Indies) and experimental approach. *Geochim. Cosmochim. Acta* **74**(6), 1852–1871.

Möller P. and Giese U. (1997) Determination of easily accessible metal fractions in rocks by batch leaching with acid cation-exchange resin. *Chem. Geol.* **137**(1–2), 41–55.

Nicollin F., Gibert D., Beauducel F., Boudon G. and Komorowski J.-C. (2006) Electrical tomography of La Soufrière of Guadeloupe Volcano, field experiments, 1D inversion and qualitative interpretation. *Earth Planet. Sci. Lett.* **244**(3–4), 709–724.

Nonell A., Toutain J.-P., Polvé M., Munoz M. and Berger G. (2005) First coupled Sr and Pb isotopic measurements in volcanic gas condensates and groundwaters of Vulcano Island (Italy). *Geochem. Geophys. Geosyst.* **6**, Q11011. http://dx.doi.org/10.1029/2005GC000980.

Pedroni A., Hammerschmidt K. and Friedrichsen H. (1999) He, Ne, Ar, and C isotope systematics of geothermal emanations in the Lesser Antilles Islands Arc. *Geochim. Cosmochim. Acta* **63**(3–4), 515–532.

Pennisi M., Leeman W. P., Tonarini S., Pennisi A. and Nabelek P. (2000) Boron, Sr, O, and H isotope geochemistry of groundwaters from Mt. Etna (Sicily) – hydrologic implications. *Geochim. Cosmochim. Acta* **64**(6), 961–974.

Petit J. C. J., De Jong J., Chou L. and Mattielli N. (2008) Development of Cu and Zn isotope MCICP-MS measurements: application to suspended particulate matter and sediments from the Scheldt Estuary. *Geostand. Geoanal. Res.* **32**(2), 149–166.

Pokrovsky O. S., Viers J. and Freydier R. (2005) Zinc stable isotope fractionation during its adsorption on oxides and hydroxides. *J. Colloid Interface Sci.* **291**(1), 192–200.

Pons M.-L., Fujii T., Rosing M., Quitté G., Télouk P. and Albarède F. (2013) A Zn isotope perspective on the rise of continents. *Geology* **11**, 201–214.

Rousteau A. (1996) Structures, flores, dynamiques, réponses des forêts pluviales des Petites Antilles aux milieux montagnards. In *Phytogéographie tropicale, réalités et perspectives* (eds. J. L. Guillaumet, M. Belin and H. Puig). ORSTOM, Paris.

Ruzié L., Moreira M. and Crispi O. (2012) Noble gas isotopes in hydrothermal volcanic fluids of La Soufrière volcano, Guadeloupe, Lesser Antilles arc. *Chem. Geol.* **304–305**, 158–165.

Salaün A., Villemant B., Gérard M., Komorowski J.-C. and Michel A. (2011) Hydrothermal alteration in andesitic volcanoes, trace element redistribution in active and ancient hydrothermal systems of Guadeloupe (Lesser Antilles). *J. Geochem. Explor.* **111**(3), 59–83.

Samper A., Quidelleur X., Komorowski J.-C., Lahitte P. and Boudon G. (2009) Effusive history of the Grande Découverte volcanic comples, southern Basse-Terre (Guadeloupe, French West Indies) from new K–Ar Cassignol-Gillot ages. *J. Volcanol. Geoth. Res.* **187**, 117–130.

Schopka H. H., Derry L. A. and Arcilla C. A. (2011) Chemical weathering, river geochemistry and atmospheric carbon fluxes from volcanic and ultramafic regions on Luzon Island, the Philippines. *Geochim. Cosmochim. Acta* **75**, 978–1002.

Symonds R. B. and Reed M. H. (1993) Calculation of multicomponent chemical equilibria in gas–solid–liquid systems: calculation methods, thermochemical data, and applications to studies of high-temperature volcanic gases with examples from Mount St. Helens. *Am. J. Sci.* **293**, 758–864.

Taran Y., Fischer T. P. and Pokrovsky B., et al. (2003) Geochemistry of the volcano-hydrothermal system of El Chichon Volcano, Chiapas, Mexico. *Bull. Volcanol.* **59**, 445–459.

Toutain J.-P., Sonke J., Munoz M., Nonell A., Polve M., Viers J., Freydier R., Sortino F., Joron J.-L. and Sumarti S. (2008) Evidence for Zn isotopic fractionation at Merapi volcano. *Chem. Geol.* **253**(1–2), 74–82.

Trémillon B. (1965) *Les séparations par les résines échangeuses d'ions*. Gauthier-Villars, Paris, 400p.

van Soest M. C., Hilton D. R. and Kreulen R. (1998) Tracing crustal and slab contributions to arc magmatism in the Lesser Antilles Island arc using helium and carbon relationships in geothermal fluids. *Geochim. Cosmochim. Acta* **62**(19–20), 3323–3335.

Varekamp J. and Thomas E. (1998) Volcanic and anthropogenic contributions to global weathering budgets. *J. Geochem. Exploit.* **62**, 149–159.

Viers J., Oliva P., Nonell A., Gélabert A., Sonke E. J., Freydier R., Gainville R. and Dupré B. (2007) Evidence of Zn isotopic fractionation in a soil–plant system of a pristine tropical watershed (Nsimi, Cameroon). *Chem. Geol.* **239**, 124–137.

Villemant B., Hammouya G., Michel A., Semet P. M., Komorowski J.-C., Boudon G. and Cheminee J.-L. (2005) The memory of volcanic waters, Shallow magma degassing revealed by halogen monitoring in thermal springs of La Soufrière volcano (Guadeloupe, Lesser Antilles). *Earth Planet. Sci. Lett.* **237**(3–4), 710–728.

Villemant B., Mouatt J. and Michel A. (2008) Andesitic magma degassing investigated through H_2O vapour-melt partitioning of halogens at Soufrière Hills volcano, Montserrat (Lesser Antilles). *Earth Planet. Sci. Lett.* **269**(1–2), 212–229.

Wilkinson J. J., Weiss D. J., Mason T. F. D. and Coles B. J. (2005) Zinc isotope variation in hydrothermal systems, preliminary evidence from the Irish midlands ore field. *Econ. Geol.* **100**(3), 583–590.

Young E. D., Galy A. and Nagahara H. (2002) Kinetic and equilibrium mass-dependent isotope fractionation laws in nature and their geochemical and cosmochemical significance. *Geochim. Cosmochim. Acta* **66**(6), 1095–1104.

Zlotnicki J., Boudon G. and Le Mouël J.-L. (1992) The volcanic activity of La Soufrière of Guadeloupe (Lesser Antilles), structural and tectonic implications. *J. Volcanol. Geoth. Res.* **49**(1–2), 91–104.

Zlotnicki J., Vargemezis G., Mille A., Bruère F. and Hammouya G. (2006) State of the hydrothermal activity of Soufrière of Guadeloupe volcano inferred by VLF surveys. *J. Appl. Geophys.* **58**(4), 265–279.

Associate editor: Jeffrey C. Alt